

Received November 13, 2018, accepted January 10, 2019, date of publication January 22, 2019, date of current version March 18, 2019.

Digital Object Identifier 10.1109/ACCESS.2019.2894175

Contactless Measurement of Hypervelocity Projectile Wake Velocity Distribution

BIXIAO JIANG¹, XIANQING YANG¹, PING MA², BO CHEN¹, JING TIAN¹, ANHUA SHI², AND PU TANG¹

¹School of Electronic Science and Engineering, University of Electronic Science and Technology of China, Chengdu 611731, China

²China Aerodynamics Research and Development Center, Hypervelocity Institute, Mianyang 621000, China

Corresponding author: Pu Tang (putang@uestc.edu.cn)

This work was supported by the Key Project of National Pre-Research Foundation through the Modelling and Measurement of Electromagnetic Scattering Characteristics of Inhomogeneous Plasma under Grant 6140416010102.

ABSTRACT This paper presents a microwave approach to investigate the wake velocity distribution of hypervelocity projectile. The ballistic range measurement is carried out to model the transport of hypervelocity object on the ground. An X-band horn antenna sends a continuous sinusoidal wave with $f_c = 8.7$ GHz to the hypervelocity object and detects the reflected signal. The continuous wavelet transform is utilized to obtain the Doppler frequency shift, and the wake velocity is calculated based on the theory of the Doppler effect. The validity of this experiment is confirmed by comparing the measured projectile velocity with that achieved by a laser-based velocity meter. As a contactless method, this approach does not interfere with the wake flow field. Therefore, the velocity distribution achieved in this paper exhibits better accuracy compared with that obtained from other contact approaches.

INDEX TERMS Contactless, hypervelocity projectile, wake, velocity.

I. INTRODUCTION

The hypervelocity projectile not only generates plasma sheath around its body but also leaves wake flow field behind. As the wake characteristics reflect significant physical properties of the high-speed object such as shape, size and velocity, it has been considered as an important approach to identify the projectile through characterizing the wake behind it.

Ballistic range, as a frequently used facility in aerodynamic research, has been widely applied to model the transport of hypervelocity object or reentering spacecraft under ambient pressure in ground test [1]. Based on this approach, S. Nonaka et al. have explored the real-gas effects of the hypervelocity target through measuring the gas density distribution of shock layer with holographic interferometry [2]. In addition, the shock standoff distance under different ambient pressure is also measured with the pulse Nd-YAG laser for various radii of sphere. In 1967, C. Lahaye et al. measured the wake velocity based on the sequential spark technique in ballistic range experiments [3]. Later in 1970, they also compared the sphere wake velocity achieved by sequential spark method with that measured by electrostatic probe, hot wire and sequential schlieren approaches [4]. Compared with the sequential schlieren technique, the rest methods are contact approaches that may destroy the wake flow field and

only record the local wake velocity. The velocity measured with sequential schlieren method is relatively lower than that achieved with other three as it measures the average velocity over the whole wake.

In this article, a microwave approach is proposed to measure the wake velocity distribution of hypervelocity projectile based on the theory of Doppler effect. As a contactless method, microwave measurement is not only applied in the characterization of plasma [5], [6], but also used in the permittivity determination of dielectrics [7], [8]. In this work, the radar antenna transmits and receives continuous sinusoidal wave in time-domain and the wake velocity is extracted from the time-frequency spectrum of the reflected signal. Wavelet transform, which is frequently used in plasma characterization [9], [10], is utilized to achieve the time-frequency spectrum. The article is arranged as follows: Section II introduces the operation principle and data analysis algorithm of the proposed approach. Section III illustrates the measurements results and Section IV concludes the paper.

II. OPERATION PRINCIPLE AND DATA ANALYSIS ALGORITHM

The setup of ballistic range measurement is shown in Fig. 1. It consists of three sections and the projectile is launched from

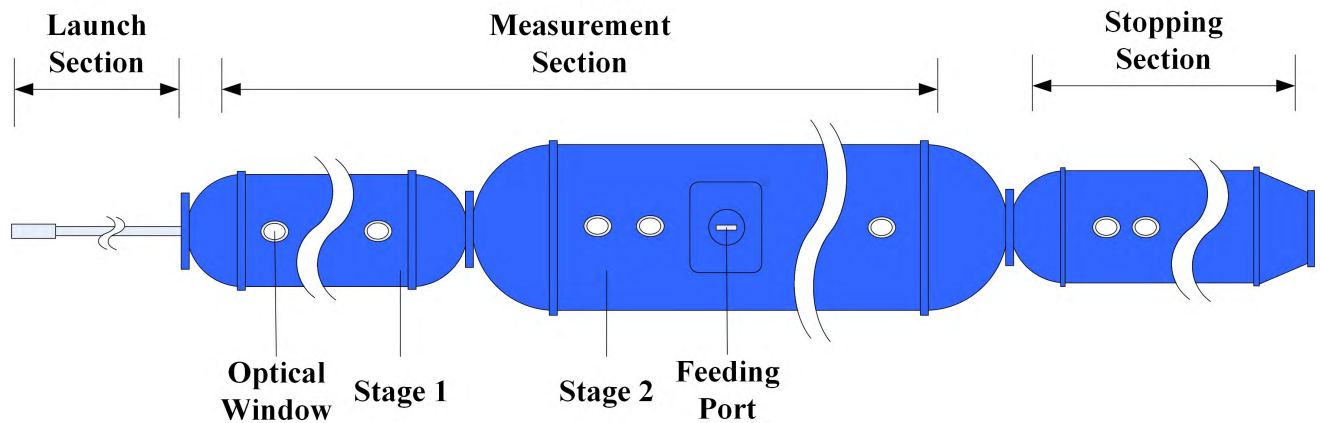


FIGURE 1. Geometry of the hypervelocity ballistic range measurement.

the launch section with three different initial velocities. The measurement section has two stages, namely, optical measurement and anechoic chamber stages. The first stage has shadow-graphing instrument and spectrometer installed to track the flying projectile and measure the radiating spectrum of the hypervelocity projectile, respectively. However, as our goal is to measure the wake velocity they remain unused in this work. A corrugated conical horn antenna operating at X-band frequencies with 20 dB gain and aperture size of 150 mm is used in the measurement. The antenna is located inside the second stage (i.e. anechoic section) with $\alpha = 43^\circ$ between the wave transmission direction and X-axis, as shown in Fig. 2, to measure the Doppler frequency shift. Hence, the velocity of the target can be calculated as:

$$V_t = \frac{cf_d}{2f_c \cos \alpha}, \quad (1)$$

where $f_c = 8.7$ GHz is the frequency of transmitted signal, f_d is corresponding Doppler frequency shift and c is the speed of light. As the experiment lasts for only a few milliseconds, it is reasonable to assume the wake velocity remains constant during this period. Hence, the extracted velocity against time at the measurement point reflects the velocity distribution of the wake.

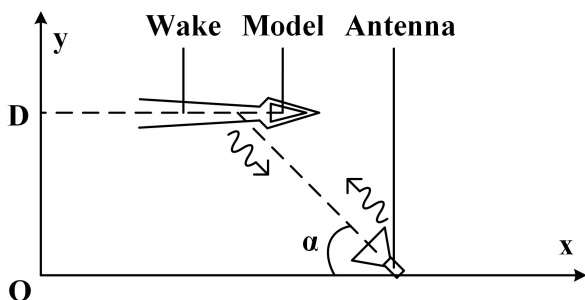


FIGURE 2. Diagram of microwave wake velocity measurement in the anechoic chamber.

The Doppler reflectometer has been widely used on tokamak facilities as a general approach to measure the rotation velocity of plasma [11]–[13]. Since the signals received are in time domain, in order to extract the corresponding Doppler frequency shift it is necessary to convert them into frequency domain. As the plasma rotates with a constant velocity in these experiments, Fourier transform (FT) were implemented to achieved the Doppler spectrum. During this process, a time-independent spectrum is achieved and time information is neglected. Hence, FT is only suitable for stationary signal without turbulence and cannot be used here to extract the time-varying Doppler frequency shift (i.e. time-frequency spectrum). In this work we utilize the continuous wavelet transform (CWT) to conduct the time-frequency analysis and extract the time-varying Doppler frequency shift caused by the wake of hypervelocity projectile.

The operation principle of CWT is to express a signal into the superposition of a few basic functions. Unlike FT that utilizes infinite sin or cos waves to reproduce the received signal, CWT chooses wavelets that are finite in time to retain the time information of received signal. The CWT for wavelet $w(\tau, a, t)$ is performed as

$$\Phi(\tau, a) = \int_{-\infty}^{\infty} s(t)w^*(\tau, a, t)dt, \quad (2)$$

where $s(t)$ is the signal and $w^*(\tau, a, t)$ is the conjugate of $w(\tau, a, t)$. If the basic function of wavelet is $h(t)$, the expression of $w(\tau, a, t)$ can be written as [14]

$$w(\tau, a, t) = \frac{1}{\sqrt{a}}h\left(\frac{t - \tau}{a}\right). \quad (3)$$

where $a = f_0/f$, f_0 is the sampling frequency, f is the frequency of interest and τ is the time that has passed since the sampling behavior starts.

According to Eq. (2), the time-frequency spectrum obtained from CWT is determined by $h(t)$. In practice, the waveform of $h(t)$ is determined according to the characteristics of the signal to be analyzed. In this work, we implement

two different wavelets (i.e. Morlet and Symmetric wavelet) to obtain the time-frequency spectrum of the reflected signal.

For Morlet wavelet,

$$h(t) = Ce^{-\frac{t^2}{2}} \cos(5t), \quad (4)$$

where C is a constant. Hence, Eq. (3) can be rewritten as

$$\begin{aligned} w(\tau, a, t) &= \frac{C}{\sqrt{a}} e^{-\frac{(t-\tau)^2}{2a^2}} \cos\left(\frac{5(t-\tau)}{a}\right) \\ &= W(\tau, a, t) \left(e^{j\frac{5(t-\tau)}{a}} + e^{-j\frac{5(t-\tau)}{a}} \right), \end{aligned} \quad (5)$$

where

$$W(\tau, a, t) = \frac{C}{2\sqrt{a}} e^{-\frac{(t-\tau)^2}{2a^2}}. \quad (6)$$

For the Symmetric wavelet, unfortunately there is no analytical expression for $h(t)$. Hence, we have to calculate the corresponding time-frequency spectrum $\Phi_S(\tau, a)$ numerically.

III. MEASUREMENT RESULTS

Fig. 3 illustrates the measured signal that has been down-converted to baseband in time domain. It is easy to see that the reflected signal is weak before the hypervelocity projectile arrives. When the target pops into the measurement window (at $\tau \approx 500 \mu\text{s}$), strong reflected signal is detected. However, the reflected signal becomes weak again after the object moves out (at $\tau \approx 900 \mu\text{s}$). The corresponding time-frequency spectrum calculated with Eq. (5) utilizing Morlet wavelet is shown in Fig. 4(a), (b) and (c). It is easy to see that three plots exhibit similar frequency distribution when the target flies through and the Doppler frequency shift caused by the projectile itself is much higher than that caused by the wake.

For the projectile with $V_p = 5076 \text{ m/s}$ (the projectile velocity used in this work are measured with the laser-based velocity meter unless otherwise stated), the strongest Doppler

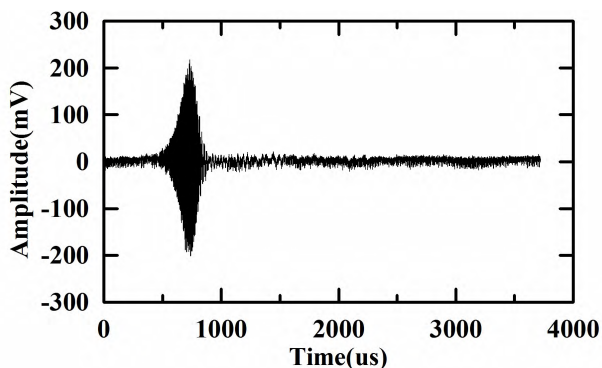


FIGURE 3. The base-band signal received for $V_p = 5076\text{m/s}$.

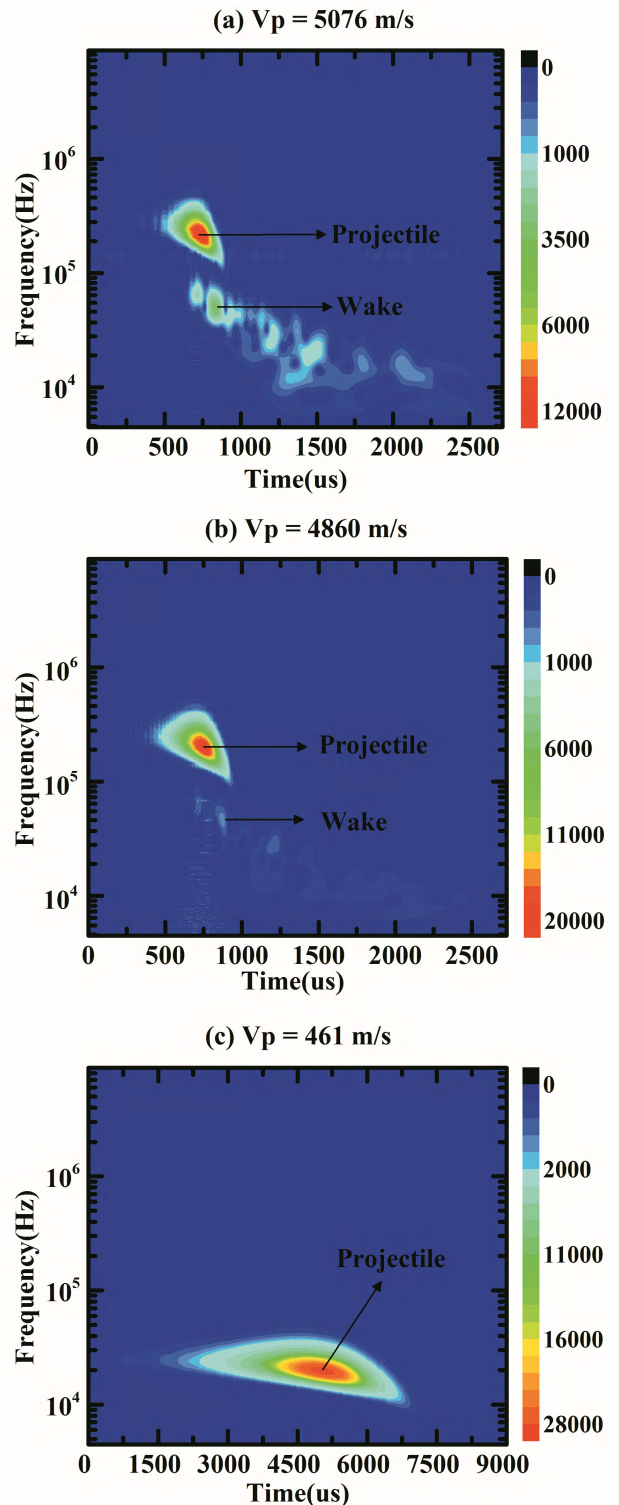


FIGURE 4. Time-frequency spectrum extracted from the reflected signals with Morlet wavelet: (a) $V_p = 5076 \text{ m/s}$; (b) $V_p = 4860 \text{ m/s}$; (c) $V_p = 461 \text{ m/s}$. The projectile velocities given here are measured by the laser-based velocity meter.

frequency shift appears at $\tau \approx 750 \mu\text{s}$ (the time when the projectile arrives at the center of beam area), in consistent with the conclusion achieved from Fig. 3. In addition, one

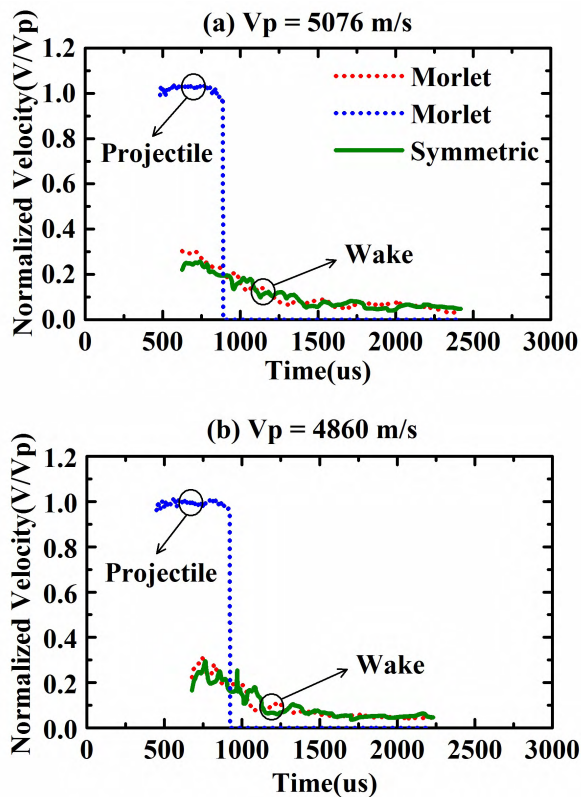


FIGURE 5. The extracted wake velocity: (a) $V_p = 5076$ m/s; (b) $V_p = 4860$ m/s.

can clearly observe the Doppler frequency shift caused by the wake behind the object between $1000 \mu s$ to $2250 \mu s$. Hence, Fig. 4(a) illustrates the presence of wake flow field behind the flying projectile that is not distinguishable in Fig. 3. That means the information that has lost in noise (see Fig. 3) is recovered by the wavelet transform. When the velocity of projectile is lower (i.e. $V_p = 4860$ m/s), it is also able to see similar strong Doppler frequency shift caused by the hypervelocity projectile but the Doppler frequency shift caused by the wake behind is weaker. For the case of $V_p = 461$ m/s, the frequency shift observed lasts much longer than the other two high-speed experiments due to the low flying speed of projectile. However, no frequency shift is observed when it moves out of the beam area due to the weak wake generated in this experiment.

To validate the proposed approach, a laser-based velocity meter is used to measure the velocity of projectile for comparison. By recording the time (t_p) projectile flies between two laser sensors, the corresponding velocity can be calculated as $V_p = d/t_p$, where d is the distance between the sensors. As the metallic projectile is reflective to microwave, the signal reflected by the projectile is much stronger compared with that reflected by the wake, which greatly increases the effective beam width and introduces an varying reflecting angle. To eliminate the errors caused by the angle variation, the projectile velocity where the strongest reflected signal

appears is calculated utilizing $\alpha = 43^\circ$ as the reference (V_r) and the velocities at $\tau = \tau_r \pm \Delta\tau$ are achieved with angles $\alpha \pm \arccos((R^2 + R_0^2 - \Delta x) / (2RR_0)) * 180/\pi$, where R_0 is the distance between antenna and the projectile for $\alpha = 43^\circ$ (see Fig. 2), $\Delta x = \Delta\tau * V_r$ and $R = \sqrt{\Delta x^2 + R_0^2 + 2 * \Delta x R_0 \cos(\alpha)}$. As Fig. 4 gives the Doppler frequency spectra for each time step rather than the Doppler frequency shifts that used for velocity calculation, it is necessary to extract the corresponding Doppler frequency shifts with the presented spectra. Take the extraction of Doppler frequency shift at the m^{th} time step $\tau = \tau_m$ in Fig. 4 (a) for example. First, the Doppler frequency spectrum at each time step is filtered with an identical highpass (or lowpass) filter when calculating the Doppler frequency shift caused by the projectile (or wake). Then, the amplitude of each frequency point within the filtered spectrum at τ_m is forced to 0 if the magnitude is lower than a predefined threshold Φ_{th} . Hence, the corresponding Doppler frequency shift at τ_m is achieved as

$$f_{d,m} = \frac{\sum_{n=1}^N \Phi(\tau_m, a_n) f_n}{\sum_{n=1}^N \Phi(\tau_m, a_n)}, \quad (7)$$

where f_n is the frequency at the n^{th} frequency point, $a_n = f_0/f_n$, $\Phi(\tau_m, a_n)$ is the magnitude of f_n at τ_m and N is the total number of frequency points that has been taken into consider at τ_m . Substitute f_d in Eq. (1) with the expression of $f_{d,m}$ given in Eq. (7), the velocity of projectile (or wake) at τ_m can be calculated.

The blue dotted lines in Fig. 5 (a) and (b) demonstrate the normalized projectile velocity achieved with the proposed approach, which demonstrates excellent agreement with results of laser-based system. Moreover, the normalized wake velocity calculated with both Morlet and Symmetric wavelets are also presented in Fig. 5 for comparison (see the red dotted and green solid lines). As the reflected signal is so weak, the effective beam width locates within a narrow region near the center of the main lobe of the horn antenna. Therefore, Eq. 1 is used to extract the wake velocity with $\alpha = 43^\circ$. The wake velocity of projectile with $V_p = 461$ m/s is not presented here due to the negligible Doppler frequency shift observed. It can be seen that the wake velocity calculated with both wavelets agree well with each other. The maximum wake velocity is approximately 30% of that of the projectile. The measured wake velocity distribution exhibits an exponentially decreasing characteristic.

IV. CONCLUSION

In summary, this paper presents a contactless approach to obtain the wake velocity distribution of hypervelocity projectile in ballistic range measurement. The wavelet transform with two different wavelets is utilized to achieve the time-frequency spectrum from which the Doppler frequency shift caused by the wake is visually presented. The validity of this method has been confirmed with a laser-based velocity meter on the velocity measurement of the projectile and the wake

shows exponentially decreasing velocity in spacial distribution. This work paves the way for hypervelocity projectile identification through wake characteristics investigation.

REFERENCES

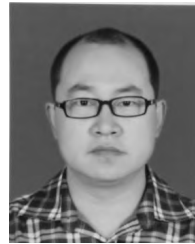
- [1] M. C. Wilder, D. W. Bogdanoff, and C. J. Cornelison, "Hypersonic testing capabilities at the NASA Ames ballistic ranges," in *Proc. 53rd AIAA Aerosp. Sci. Meeting*, 2015, p. 1339.
- [2] S. Nonaka, T. Hashimoto, M. Furudate, and K. Takayama, "Measurement of density distribution over a hemisphere in ballistic range," *J. Thermophys. Heat Transf.*, vol. 25, no. 3, pp. 464–468, 2011.
- [3] C. Lahaye, E. G. Leger, and A. Lemay, "Wake velocity measurements using a sequence of sparks," *AIAA J.*, vol. 5, no. 12, pp. 2274–2276, 1967.
- [4] H. Doyle, L. Jean, and C. Lahaye, "Velocity distributions in the wake of spheres," *AIAA J.*, vol. 8, no. 8, pp. 1521–1523, 1970.
- [5] F. Skiff, "Diagnostics of collisionless processes in plasma," *IEEE Trans. Plasma Sci.*, vol. 34, no. 4, pp. 1548–1552, Aug. 2006.
- [6] J. Tian *et al.*, "Single-frequency reflection characterisation of shock tube excited plasma," *AIP Adv.*, vol. 7, no. 8, p. 085115, 2017.
- [7] K. Xu *et al.*, "Novel microwave sensors based on split ring resonators for measuring permittivity," *IEEE Access*, vol. 6, pp. 26111–26120, 2018.
- [8] L. Li, H. Hu, P. Tang, R. Li, B. Chen, and Z. He, "Compact dielectric constant characterization of low-loss thin dielectric slabs with microwave reflection measurement," *IEEE Antennas Wireless Propag. Lett.*, vol. 17, no. 4, pp. 575–578, Apr. 2018.
- [9] K. Ghanbari, M. Ghoranneviss, A. Elahi, A. Salar, and S. Saviz, "X-ray irradiation analysis based on wavelet transform in tokamak plasma," *J. X-Ray Sci. Technol.*, vol. 22, no. 6, pp. 777–783, 2014.
- [10] M. Sabouri, S. M. M. Khoei, and J. Neshati, "Plasma current analysis using discrete wavelet transform during plasma electrolytic oxidation on aluminum," *J. Electroanal. Chem.*, vol. 792, pp. 79–87, May 2017.
- [11] K. D. Lee, Y. U. Nam, S.-H. Seo, and Y. S. Kim, "Design of a Doppler reflectometer for KSTAR," *Rev. Sci. Instrum.*, vol. 85, no. 11, p. 11D858, 2014.
- [12] T. Tokuzawa *et al.*, "Microwave Doppler reflectometer system in LHD," *Rev. Sci. Instrum.*, vol. 83, no. 10, p. 10E322, 2012.
- [13] C. Zhou *et al.*, "Microwave Doppler reflectometer system in the experimental advanced superconducting tokamak," *Rev. Sci. Instrum.*, vol. 84, no. 10, p. 103511, 2013.
- [14] O. Rioul and M. Vetterli, "Wavelets and signal processing," *IEEE Signal Process. Mag.*, vol. 8, no. 4, pp. 14–38, Oct. 1991.



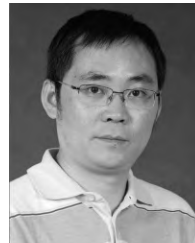
BIXIAO JIANG received the B.S. degree in electromagnetic field and wireless technique from the University of Electronic Science and Technology of China, Chengdu, Sichuan, China, in 2016, where he is currently pursuing the M.S. degree in electronic and communication engineering. His research interests include the electromagnetic scattering of plasma.



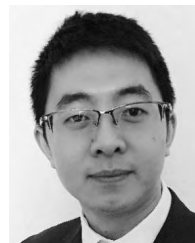
XIANQING YANG was born in China, in 1956. He is currently a Professor with the School of Electronic Science and Engineering, University of Electronic Science and Technology of China. His major research interests include electromagnetic compatibility.



PING MA is currently a Senior Engineer with the China Aerodynamics Research and Development Center, Hypervelocity Institute. His major research interests include the electromagnetic scattering of hypervelocity targets, the communication interrupt of hypervelocity crafts, and plasma diagnosis.



BO CHEN received the B.S. degree from the University of Electronic Science and Technology of China, where he is currently an Associate Professor. His research interests include microwave and millimeter wave measurements, antenna design, and electromagnetic compatibility and protection.



JING TIAN received the M.S. degree from the Tampere University of Technology, Finland, and the Ph.D. degree from the Queen Mary University of London, U.K. He is currently a Lecturer with the University of Electronic Science and Technology of China. His research interests include graphene and other 2D materials-based electromagnetic devices and field-effect transistors, microwave measurements, plasma characterization, and electromagnetic compatibility and protection.



ANHUA SHI is currently a Researcher of the China Aerodynamics Research and Development Center, Hypervelocity Institute. His current research interests include the optical radiation and spectral characteristics of hypervelocity targets and the optical radiation of hypervelocity impacts.



PU TANG received the M.S. degree from the University of Electronic Science and Technology of China, where he is currently a Professor. His research interests include microwave and millimeter wave measurements, plasma characterization, antenna design, and electromagnetic compatibility.

...